

Comparative study of classical and DFT modelisation of amorphous TiO_2 nanoparticles

Nicolas Gastellu¹ and Rustam Z. Khaliullin^{1,*}

¹*Department of Chemistry, McGill University, 801 Sherbrooke St. West, Montreal, QC H3A 0B8, Canada*

(Dated: September 4, 2018)

We calculate the energy of various conformations of amorphous titania nanoparticles (obtained using classical MD simulations) using the classical two-body MA potential and traditional KS DFT. Comparing the energies we obtained for each configuration, through both calculation methods, lead to the observation that the set of values obtained using a classical formalism was only weakly correlated with the energy values returned by DFT. Even systems which were expected to be well parameterised by the MA potential (in our case, an $r - \text{TiO}_2$ nanocrystal) exhibited almost no correlation between both sets of calculated energies. We discuss possible reasons for this discrepancy between both calculation methods in and conclude by examining the questions raised by our results; chief among them are the suitability of the classical picture for $a - \text{TiO}_2$ nanoparticles and the necessity of DFT-level precision in computational simulations of such systems.

INTRODUCTION

Titania (TiO_2) has long been the subject of notable research interest due to its high chemical stability and interesting optical, dielectric, mechanical, and photocatalytic properties^{1–4}. While most works focus on TiO_2 in its most stable and common forms, which are all crystalline, a number of technological uses of this material rely on processing into film or powder form which both tend to be amorphous; further modification of the material is then needed to restore a certain level of crystalline order back to it^{5,6}. Dependence on this last step makes titania significantly more difficult and expensive to use in industrial-scale applications, which has motivated researchers to study amorphous TiO_2 ($a - \text{TiO}_2$) in hope of being able to use in it cheaper, less processed forms^{7–9}.

One of the defining traits of amorphous materials is their lack of long-range order, which makes their microstructure extremely hard to study experimentally. In spite of this, recent experimental studies have been successful in describing the local atomic structure of $a - \text{TiO}_2$ under different environments^{10–12} by measuring things like the coordination number of bulk and surface Ti atoms and average bond lengths, using various types of X-ray absorption structure spectroscopy. However, the most detailed investigations of amorphous titania’s structure have been those combining experimental methods (e.g. X-ray absorption spectroscopy) with the computation modeling (notably reverse Monte-Carlo simulations)^{13–15}. Our reliance on simulations to properly understand this material is a major research incentive for theoretical chemists to devise the computational tools to perform such simulations adequately.

Seeing as $a - \text{TiO}_2$ nanoparticles are almost always used for inhomogeneous catalysis purposes, it is often needed to simulate their structure’s evolution over time (e.g. the duration of a given reaction or phase transition). This is the purview of molecular dynamics (MD) simulations. There exist two approaches to MD simulations:

- the classical approach, which uses a predetermined potential $V(\mathbf{r}_1, \dots, \mathbf{r}_N)$ and Newton’s equations of motion to calculate the trajectories and energies of all atoms in the simulation,
- the *ab-initio* approach, which relies on a quantum mechanical description (usually density functional theory, or DFT) of the system to determine its electronic density from which all other physical quantities are then derived.

It is known that DFT is more accurate than classical simulations, due to its more faithful description of interactions between each atoms in the system being studied. Unfortunately, DFT simulations of large systems (~ 1000 atoms) are much more difficult to implement due to the prohibitive amounts of memory needed and long computation times. Researchers have therefore put considerable effort into developing classical potentials that faithfully reproduce experimental measurements which could allow accurate simulations of TiO_2 (notably) without resorting to computationally expensive calculations^{16–18}. The potential devised by Matsui and Akaogi in 1991¹⁷ has had notable success in describing the structural and mechanical properties of titania’s different polytypes^{19,20} and is thus the most widely used potential when simulating TiO_2 using classical MD. In this work, we focus our attention on nanoparticulate $a - \text{TiO}_2$ (such as can be found in unprocessed powder form) and on whether this classical potential can accurately predict their structure-energy relationship, or potential energy surface (PES) $V(\mathbf{r}_1, \dots, \mathbf{r}_N)$. We compare the energies yielded by the classical and quantum descriptions of the system to see how well correlated they are. In this paper, we begin by describing our different calculation methods, then we present and discuss our results, before introducing potential directions for future research.

TABLE I. Parameters used for evaluating the MA potentials.

Element	Z ($ e $)	A (\AA)	B (\AA)	C ($\text{\AA}^3 \text{kJ}^{1/2} \text{mol}^{-1/2}$)
Ti	+2.196	1.1823	0.077	22.5
O	-1.098	1.6339	0.117	54.0

I. SIMULATION DETAILS

The open-source atomistic simulations package CP2K²¹ was used to run all calculations and simulations presented in this work.

A. Classical MD

All classical MD simulations described in this work were ran in the NpT ensemble, using the Matsui-Akaogi (MA) potential to model the interactions between pairs of atoms. The MA potential was originally developed for classical MD simulations of the four main polytypes of crystalline TiO_2 ¹⁷ to accurately simulate the structural properties of titania's four main polytypes and the elastic constants of rutile ($r - \text{TiO}_2$). It is the most widely used potential when classically simulating bulk TiO_2 and has been shown by previous studies^{19,20,22} to be the most adequate force field for predicting the structure and properties of its liquid and amorphous phases. The MA potential describes the short-range interaction between atoms with a Buckingham potential and their long-range electrostatic interaction using the traditional Coulomb term:

$$V_{ij}(r) = f_0 \cdot (B_i + B_j) \cdot \exp\left(\frac{A_i + A_j - r}{B_i + B_j}\right) - \frac{C_i C_j}{r^6} + \frac{e Z_i Z_j}{4\pi\epsilon_0 r}, \quad (1)$$

where r denotes the distance between the two interacting ions i and j , e is the elementary charge, Z_i is the dimensionless ionic charge of ion i , f_0 is a standard force of $4.184 \text{ kJmol}^{-1} \text{\AA}^{-1}$, and A_i , B_i , and C_i are parameters corresponding to species i . The charges Z_{Ti} and Z_{O} were obtained from Traylor *et al.*²³, who derived them from phonon dispersion curves he observed in rutile ($r - \text{TiO}_2$). The numerical values of the other constants listed above were determined by Matsui and Akagi by adjusting them to reproduce the observed elastic constants of rutile and fitting them to reproduce the structures of rutile, brookite, and anatase (the three polytypes of crystalline titania for which precise experimental measurements of lattice parameters were available at the time of their paper). These values are given in table I. The total potential energy of the system is then given by the sum of all pairwise interactions between all of its N atoms:

$$V(\mathbf{r}_1, \dots, \mathbf{r}_N) = \sum_{i < j}^N V_{ij}(|\mathbf{r}_i - \mathbf{r}_j|). \quad (2)$$

The atomic structures of the various $a - \text{TiO}_2$ nanoparticles described in this work were obtained in multiple steps, using the melt-quenching method employed by a number of computational studies of amorphous materials^{6,24}. We started by melting rutile ($r - \text{TiO}_2$) nanocrystals of 198, 390, and 768 atoms respectively whose structures were previously optimized *via* DFT at the BLYP/DZVP level of theory (with a plane-wave energy cutoff of 2100 Ry) using classical MD in the NpT ensemble with $T = 2000 \text{ K}$ and $p_{\text{ext},0} = 0.0 \text{ Pa}$. We ran this first round of simulations for 40000 timesteps of $\Delta t = 0.5 \text{ fs}$. The resulting melt was then cooled in three steps; classical MD simulations using the same potentials, ensemble, and number of steps were ran using $T = 1500 \text{ K}$, 750 K , and 300 K successively, all with $\Delta t = 2.0 \text{ fs}$. This process simulated the annealing of the melted nanocrystals into a glass which we then studied using Kohn-Sham DFT.

Seeing as the MA potential was originally elaborated to describe the structural and elastic properties of $r - \text{TiO}_2$, we also generated a set of conformations of a rutile lattice comprised of 72 atoms in the NpT ensemble at $T = 300 \text{ K}$, using the same potential as described above. Doing so provided us with energy values which we expect to be well correlated with the ones we obtain with DFT methods, thus giving us a reference data set to which we could compare the rest of our results.

B. DFT calculations

Having obtained equilibrated atomic structures for nanoparticles of different sizes, we sampled 101 conformations from the last 40 ps of the last cooling run, at which point all four nanoparticles were in equilibrium with $T = 300 \text{ K}$ thermal bath. We then ran a single-point energy calculation on each conformation using traditional Kohn-Sham (KS) DFT in the generalised gradient approximation (GGA), with the fully non-empirical functional developed by Perdew, Burke, and Ernzerhof²⁵ (i.e. the PBE functional). We employed a double-zeta valence polarised (DZVP) basis set, with a plane-wave cutoff of 2000 Ry. This was all implemented using CP2K's Quickstep module for DFT calculations²⁶. We also ran similar DFT calculations on the different configurations of the reference rutile lattice which we also sampled from the last 40 ps of the MD simulation we mentioned in the last paragraph of the last section.

Seeing as core electrons have been shown to have a negligible impact on the interatomic interactions in TiO_2 ^{15,27} (especially at $p = 0 \text{ Pa}$), we used norm-conserving pseudopotentials developed by Goedecker, Teter, and Hutter²⁸ to avoid having to explicitly account for them in our electronic density optimisation routine, thereby making our *ab-initio* calculations significantly computationally cheaper. The GTH pseudopotentials used in this study treated oxygen's $1s$ orbitals as part

of its core and included all but titanium's $3p$, $3d$, and $4s$ electrons into titanium's core.

II. RESULTS AND DISCUSSION

A. Accuracy of KS DFT results

Before discussing the accuracy of our classically obtained energy values, we must first establish the accuracy of our DFT energy values for each system, since these values will serve as references to which we will compare the energies returned by the classical MD simulation. One of the main reasons why we expect our DFT results to be more realistic than the ones yielded by the classical MD simulations is that DFT's quantum formalism is better suited to describe systems at an atomic scale than the classical picture. Indeed, while classical mechanics remain a valid description of macroscopic systems (containing $\sim 10^{24}$ atoms), they do not apply to the behaviour of individual atoms, which are quantum objects (i.e. do not evolve deterministically and thus have to be described using time-evolving probability distributions). Seeing as both methods implemented in this work describe the forces in amorphous TiO_2 nanoparticles atom by atom, it is safe to assume that the procedure rooted in the most accurate theoretical substrate (for describing microscopic systems) yields better results. Furthermore, classical MD simulation rely on a fixed expression for the system's PES, whose parameters are empirically determined and thus subject to experimental error. Another problem with the potential we used for our classical MD runs is the fact that its parameters been tailored to reproduce the structures and properties of crystalline titania whereas we are trying to verify its accuracy for $a - \text{TiO}_2$.

Going beyond merely conceptual arguments for assuming that our DFT results are more accurate than those we obtained using classical MD, we note that KS DFT has been extensively used to study amorphous and crystalline titania in various forms and environments with good success^{6,27,29,30}. DFT methods thus have a proven track record of correctly reproducing experimentally observed properties, which further comforts our assumption that the energy values we calculating using DFT are a good reference to which we can compare our classical results.

Finally, our DFT calculations have converged quickly in the majority of cases and have overall exhibited good numerical behaviour (e.g. no radical changes in energy from one iteration to the next, quasi-uniformly decreasing convergence and total energy over the entire length of the calculation). Figure 1 shows the convergence of a DFT calculation made on a conformation the 72-atom $r - \text{TiO}_2$ nanocrystal (in blue). As is clearly visible, the convergence steadily decreases as the calculation progresses thereby implying that the changes being made to the computed energy value are getting smaller with each iteration of the DFT energy calculation rou-

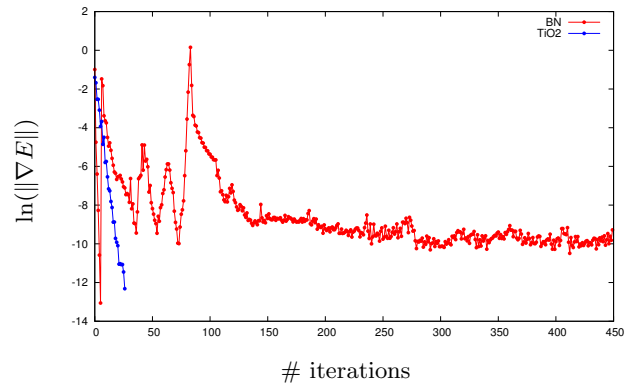


FIG. 1. Logarithmic plot of convergence vs number of iterations for a conformation of the $r - \text{TiO}_2$ nanoparticle. The convergence for a similar DFT calculation on another system (crystalline boron nitride) showing much more numerical instability is shown in red, for comparison purposes.

time. This behaviour suggests that the calculation does not exhibit significant numerical error and that the result it outputs is very likely physical.

B. Comparing classical MD with KS DFT

For each nanoparticle, we compare the classically evaluated energy of every configuration with the energy obtained through a DFT calculation for that some configuration. We plot our results in figures 2-6; a $y = x$ line was added to every plot to give a better appreciation of the level of correlation between classical and DFT data sets. This allows us to gauge the accuracy of MA force-field; if the classical and quantum mechanical results are well correlated, then the purely classical representation of the forces in the nanoparticles is sufficiently accurate to discriminate between slight variations in a given system's configuration in a meaningful way and can therefore be used to simulate this system nanoparticles instead of DFT, which is much more computationally expensive.

Comparing the energies obtained using classical MD and those calculated using DFT reveals that a description of the forces inside an $a - \text{TiO}_2$ nanoparticle using only the two-body MA potential is not precise enough to yield an accurate representation of its potential energy surface (PES) (with respect to its atoms' positions). Indeed, plotting the energies yielded by both calculation methods reveals that DFT calculation methods are much more sensitive to a change in a given nanoparticle's atomic configuration than classical methods.

The system for which this is the most obvious is the 768 atom nanoparticle, for which all classically evaluated energies lie within $\sim 10^{-4}$ Ha of each other, while the energies obtained using quantum mechanical methods vary by $\sim 10^{-1}$ Ha. One can get a sense of how dramatic this disparity between the ranges of of both

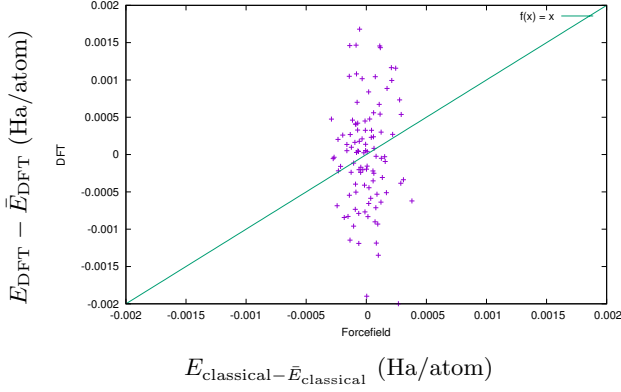


FIG. 2. DFT energy vs. classical energy (both shifted down by their average value) for 101 conformations of an r - TiO_2 lattice with 72 atoms.

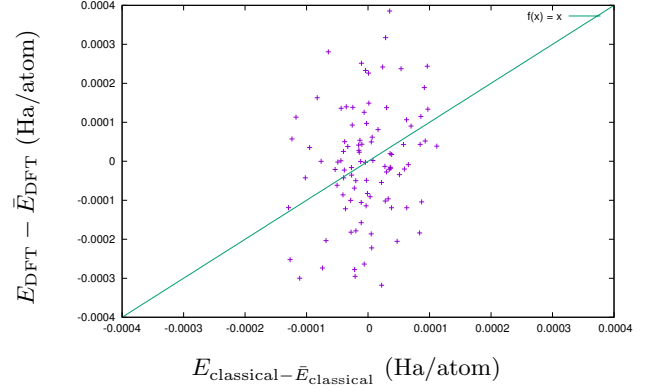


FIG. 4. DFT energy vs. classical energy (both shifted down by their average value) for 101 conformations of an a - TiO_2 nanoparticle with 390 atoms.

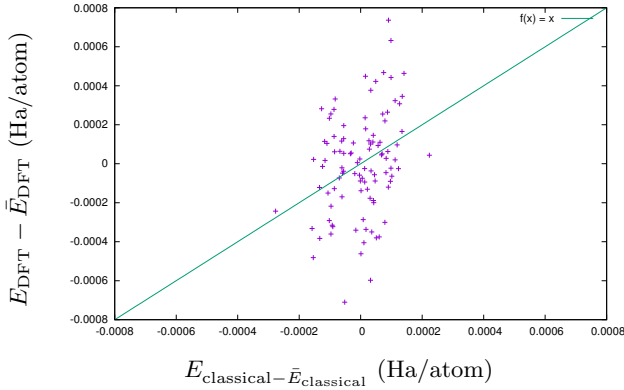


FIG. 3. DFT energy vs. classical energy (both shifted down by their average value) for 101 conformations of an a - TiO_2 nanoparticle with 198 atoms.

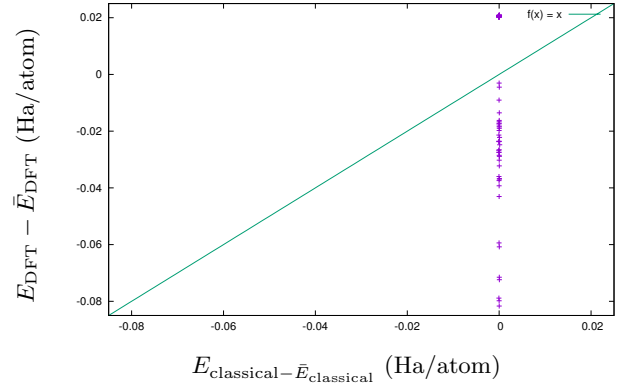


FIG. 5. DFT energy vs. classical energy (both shifted down by their average value) for 101 conformations of an a - TiO_2 nanoparticle with 768 atoms.

data sets by examining figure 5: when plotting the DFT and classical data on the same scale, the classical energy values almost all lie on the same vertical line and thus appear to all be identical. While this effect is most dramatic for the 768 atom system, every other nanoparticle on which we ran similar calculations exhibit significant clustering of the energies obtained using the MA potential about their mean value, while their DFT energies spread out over a much larger interval.

All four nanoparticles we ran these calculations exhibit weak correlation between the DFT-calculated energy values and the energies obtained using the MA potential. Even more surprisingly we find that the two sets of energy values of the different conformations of the rutile lattice were even less correlated than the ones obtained from the amorphous nanoparticles. Indeed, as can be seen in table II B, our simulated rutile lattice yielded the lowest value of ρ of all the systems we studied.

In light of this extremely low correlation, we obviously cannot consider our simulated r - TiO_2 lattice a reference system. This unexpectedly poor correlation

between these two sets of energy values also questions the accuracy of our DFT results, which have been our accuracy benchmark throughout this paper. Assuming for now that our DFT calculations are indeed accurate, this lack of correlation between the energies obtained from r - TiO_2 is not overly problematic; it could simply suggest that a purely classical two-body description of atomic interactions in TiO_2 in the amorphous or rutile phase is not sufficiently accurate to keep track of small changes in the system's configuration. Moreover the small RMSE values we get for all systems (except the 768-atom nanoparticle) and the fact that all classically obtained energies for a given system are very close to each other suggest that they are still physically sound at a less precise level of analysis. Indeed, if both sets of energy values for each system varied over intervals of similar sizes and yet remained as uncorrelated as we have observed them to be, then the validity of trying to describe TiO_2 using only the MA potential would be seriously questioned. However this is not the case; for every system all energies computed classically differ very little.

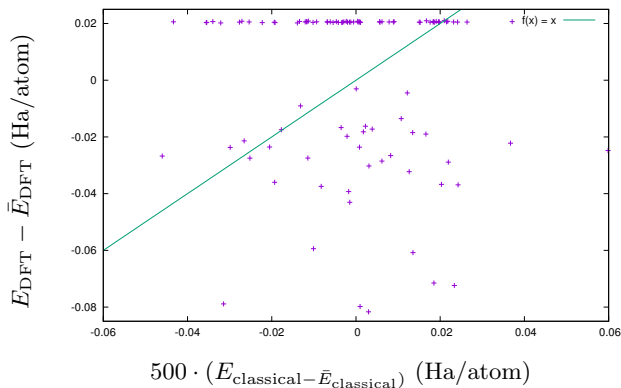


FIG. 6. Rescaled version of figure 5.

This is consistent with the fact that the atomic configurations from which such energies are computed were obtained from segments of our MD simulations where the system was already at equilibrium with its environment (i.e. the thermal bath) and thus did not vary greatly either. It is therefore reassuring to see that, within our classical MD simulation, snapshots which have similar structures are also predicted to have close energy values. The contrast between the highly clustered classical values and the much more spread out quantum values could therefore suggest that the quantum description of TiO_2 is much more sensitive to the system's conformational changes while using the MA potential cannot meaningfully register such changes yet still provides an internally consistent and physically viable picture of the system.

As stated in the previous paragraph, it could also be possible that the results we obtained *via* DFT are inaccurate. While this is unlikely (see previous subsection), a few different factors could be responsible for corrupting our DFT data. One of the most plausible hypotheses is that we obtained our classical energy values from an MD simulation with $T = 300$ K while our DFT routine calculates the ground state energy of a system at $T = 0$ K. This discrepancy between the assumptions made by both calculation methods could explain why our energy values for our simulated $r - \text{TiO}_2$ nanostructures are so weakly correlated.

Another possible explanation for the uncorrelatedness of the $r - \text{TiO}_2$ energy sets is our simulated lattice's small size. As previously stated, the MA potential was developed to reproduce the bulk structures of TiO_2 in its various crystalline forms; the potential was developed by simulating nanocrystals ranging from 384 atoms to 576 atoms in size and the bulk properties of the different crystalline polytypes of titania were used to fix its energy parameters. Knowing that the surface sites of a TiO_2 nanoparticle (crystalline or amorphous) have significantly different atomic and electronic structures as bulk sites^{20,29,31}, it is easy to see how a model built to simulate systems containing mainly bulk sites can reach erroneous results when trying to reproduce a nanoparticle

with a significant portion of its atoms on the surface. A classical MD simulation of a larger $r - \text{TiO}_2$ lattice would probably yield a better set of reference conformation and energy values. Unfortunately, running DFT single-point energy calculations on larger nanoparticles might prove to be prohibitively computationally expensive without optimising the DFT calculation scheme to handle systems with many atoms (> 1000 atoms). Regardless of how well the MA potential describes $r - \text{TiO}_2$, the data we obtained from modeling amorphous systems unequivocally indicates that the MA potential is not accurate enough to reproduce their PES adequately.

CONCLUSION

Our comparison of the energy values we obtained through DFT and those calculated with the classical MA potential, on common sets of conformations of various TiO_2 nanoparticles has consistently revealed that these two data sets are weakly correlated. Having established our DFT results to be more accurate than the ones yielded by the MA potential, we can safely assume that the MA potential does not faithfully reproduce the PES of small titania nanoparticles. This holding true even for the set of energies obtained from a system which we believed to be well-described by both methods – a 72-atom rutile nanocrystal – raises some questions about the validity of our results and calls for further research into this topic.

Conducting a similar study on larger nanoparticles could provide further insight. Indeed, the structure and properties of large nanoparticles are less impacted by their surface sites than smaller nanoparticles. Computational expense being one of DFT's main drawbacks, a number of optimisation schemes have been proposed over the years to reduce both the amount of memory and the time necessary to run calculations on large systems (~ 1000 atoms). Among them, the absolutely localised molecular orbitals³² (ALMO) method partitions the simulated system into small fragments (usually these are the individual atoms or molecules that compose it) and runs traditional DFT on each fragment in parallel. This has the advantage of having a runtime that scales linearly with the number of fragments for large systems, while traditional DFT calculation runtimes scale cubically with the number of atoms being simulated. Seeing as ALMO DFT makes a number of large DFT calculations much more feasible, it would allow us to conduct a similar study on larger nanoparticles (with more bulk sites) which could potentially yield better correlated classical and DFT values. This could furthermore enable us to run simulations of nanoparticles with sizes closer to those of $a - \text{TiO}_2$ nanoparticles used in most practical applications ($\sim 4 \text{ nm}^{29}$) and therefore give us a better appreciation of how the MA potential performs on systems it is better adapted to model.

Another way to run similar calculations on

System	$a - \text{TiO}_2$ (198 atoms)	$a - \text{TiO}_2$ (390 atoms)	$a - \text{TiO}_2$ (768 atoms)	$r - \text{TiO}_2$ (72 atoms)
ρ	0.3066474	0.3497706	-0.0496755	0.0141203
RMSE	0.0486056	0.0628487	22.21090	0.0518275

TABLE II. Pearson correlation coefficient ρ and RMSE between the energy values obtained through DFT and those obtained using the two-body MA potential on various configurations of different systems.

larger TiO_2 nanoparticles would be use smaller basis sets. While the basis set we used to describe oxygen's electronic distribution (DZVP) cannot be further reduced without removing a polarisation function (which is crucial to adequately describe chemical bonding), the basis set we used for Ti explicitly describes the electrons in its three highest occupied subshells ($3p$, $3d$, and $4s$). Knowing that we can safely assume that titanium's six $3p$ electrons have negligible impact on bonding in TiO_2 ²⁷, we can use a basis set and pseudopotential which treat them as core electrons. This would significantly reduces the memory cost and computation time of a DFT simulation of any system containing numerous Ti atoms, thus making DFT calculations on large TiO_2 nanoparticles more easily feasible.

Being able to carry out cheap DFT calculations could eventually allow for full MD simulations of nanoparticulate titania using DFT. This would give researchers the means to generate atomic structures of TiO_2 nanoparticles from first principles only. Comparing these *ab-initio* structures' properties (e.g. density, bulk/surface coordination number, average bond length) to those of structures obtained through experiment or using classical potentials might also offer insight on how well-suited both simulations methods are to describing such systems. Implementations of DFT that are optimised for large systems could also be used to study the size dependence of many of nanoparticulate titania's properties and to examine whether our current models can adequately account for them.

[CONCLUDING REMARKS]

* rustam.khaliullin@mcgill.ca

- ¹ P. A. Christensen, A. Dilks, T. A. Egerton, and J. Temperley, "Infrared spectroscopic evaluation of the photodegradation of paint part ii: The effect of uv intensity & wavelength on the degradation of acrylic films pigmented with titanium dioxide," *Journal of Materials Science* **35**, 5353–5358 (2000).
- ² K.A. Vorotilov, E.V. Orlova, and V.I. Petrovsky, "Sol-gel tio2 films on silicon substrates," *Thin Solid Films* **207**, 180 – 184 (1992).
- ³ AJ Perry and HK Pulker, "Hardness, adhesion and abrasion resistance of tio2 films on glass," *Thin Solid Films* **124**, 323–333 (1985).
- ⁴ Yi Ma, Xiuli Wang, Yushuai Jia, Xiaobo Chen, Hongxian Han, and Can Li, "Titanium dioxide-based nanomaterials for photocatalytic fuel generations," *Chemical reviews* **114**, 9987–10043 (2014).
- ⁵ Hengbo Yin, Yuji Wada, Takayuki Kitamura, Shingo Kambe, Sadao Murasawa, Hirotaro Mori, Takao Sakata, and Shozo Yanagida, "Hydrothermal synthesis of nano-sized anatase and rutile tio2 using amorphous phase tio2," *Journal of Materials Chemistry* **11**, 1694–1703 (2001).
- ⁶ Binay Prasai, Bin Cai, M. Kylee Underwood, James P. Lewis, and D. A. Drabold, "Properties of amorphous and crystalline titanium dioxide from first principles," *Journal of Materials Science* **47**, 7515–7521 (2012).
- ⁷ Jian Zou, Jiacheng Gao, and Fengyu Xie, "An amorphous tio2 sol sensitized with h2o2 with the enhancement of photocatalytic activity," *Journal of Alloys and Compounds* **497**, 420–427 (2010).
- ⁸ Miki Kanna, Sumpun Wongnawa, Supat Buddee, Ketsarin Dilokkhunakul, and Peerathat Pinpithak, "Amorphous titanium dioxide: a recyclable dye remover for water treatment," *Journal of sol-gel science and technology* **53**, 162–170 (2010).
- ⁹ Hu Young Jeong, Jeong Yong Lee, and Sung-Yool Choi, "Interface-engineered amorphous tio2-based resistive memory devices," *Advanced Functional Materials* **20**, 3912–3917 (2010).
- ¹⁰ Vittorio Luca, Samitha Djajanti, and Russell F Howe, "Structural and electronic properties of sol- gel titanium oxides studied by x-ray absorption spectroscopy," *The Journal of Physical Chemistry B* **102**, 10650–10657 (1998).
- ¹¹ Hideaki Yoshitake, Tae Sugihara, and Takashi Tatsumi, "Xafs study on the local structure of ti in amorphous mesoporous titania," *Physical Chemistry Chemical Physics* **5**, 767–772 (2003).
- ¹² Marcos Fernández-García, Carolina Belver, Jonathan C Hanson, Xianqin Wang, and José A Rodriguez, "Anatase-tio2 nanomaterials: Analysis of key parameters controlling crystallization," *Journal of the American Chemical Society* **129**, 13604–13612 (2007).
- ¹³ V Petkov, G Holzhüter, U Tröge, Th Gerber, and B Himmel, "Atomic-scale structure of amorphous tio2 by electron, x-ray diffraction and reverse monte carlo simulations," *Journal of non-crystalline solids* **231**, 17–30 (1998).
- ¹⁴ Hengzhong Zhang, Bin Chen, Jillian F Banfield, and Glenn A Waychunas, "Atomic structure of nanometer-sized amorphous tio 2," *Physical Review B* **78**, 214106 (2008).
- ¹⁵ C. A. Triana, C. Moyses Araujo, R. Ahuja, G. A. Niklasson, and T. Edvinsson, "Electronic transitions induced by short-range structural order in amorphous tio2," *Phys. Rev. B* **94**, 165129 (2016).
- ¹⁶ Dae-Weon Kim, Naoya Enomoto, Zenbe-e Nakagawa, and Katsuyuki Kawamura, "Molecular dynamic simulation in titanium dioxide polymorphs: Rutile, brookite, and anatase," *Journal of the American Ceramic Society* **79**,

- 1095–1099 (1996).
- ¹⁷ Masanori Matsui and Masaki Akaogi, “Molecular dynamics simulation of the structural and physical properties of the four polymorphs of tio_2 ,” *Molecular Simulation* **6**, 239–244 (1991).
- ¹⁸ Erik G Brandt and Alexander P Lyubartsev, “Systematic optimization of a force field for classical simulations of tio_2 –water interfaces,” *The Journal of Physical Chemistry C* **119**, 18110–18125 (2015).
- ¹⁹ DR Collins and W Smith, *Daresbury Research Report DL-TR-96-001: Evaluation of TiO_2 forcefields.*, Tech. Rep. (Council for the Central Laboratory of Research Councils, 1996).
- ²⁰ Vo Van Hoang, “Structural properties of simulated liquid and amorphous tio_2 ,” *physica status solidi (b)* **244**, 1280–1287 (2007).
- ²¹ CP2K Developers Group, “2K open source molecular dynamics: www.cp2k.org,” (—2018—).
- ²² Mozhgan Alimohammadi and Kristen A Fichthorn, “Molecular dynamics simulation of the aggregation of titanium dioxide nanocrystals: preferential alignment,” *Nano letters* **9**, 4198–4203 (2009).
- ²³ Joseph Gibson Traylor, HG Smith, RM Nicklow, and MK Wilkinson, “Lattice dynamics of rutile,” *Physical Review B* **3**, 3457 (1971).
- ²⁴ DA Drabold, “Topics in the theory of amorphous materials,” *The European Physical Journal B* **68**, 1–21 (2009).
- ²⁵ J. P. Perdew, K. Burke, and M. Ernzerhof, “Generalized gradient approximation made simple,” *Phys. Rev. Lett.* **77**, 3865 (1996).
- ²⁶ J. Vandevondele, M. Krack, F. Mohamed, M. Parrinello, T. Chassaing, and J. Hutter, “Quickstep: Fast and accurate density functional calculations using a mixed gaussian and plane waves approach,” *Comput. Phys. Commun.* **167**, 103 (2005).
- ²⁷ M Landmann, E Rauls, and WG Schmidt, “The electronic structure and optical response of rutile, anatase and brookite tio_2 ,” *Journal of physics: condensed matter* **24**, 195503 (2012).
- ²⁸ S Goedecker, M Teter, and Jürg Hutter, “Separable dual-space gaussian pseudopotentials,” *Physical Review B* **54**, 1703 (1996).
- ²⁹ Daniele Selli, Gianluca Fazio, and Cristiana Di Valentin, “Using density functional theory to model realistic tio_2 nanoparticles, their photoactivation and interaction with water,” *Catalysts* **7**, 357 (2017).
- ³⁰ E Shojaee and MR Mohammadizadeh, “First-principles elastic and thermal properties of tio_2 : a phonon approach,” *Journal of Physics: Condensed Matter* **22**, 015401 (2009).
- ³¹ VV Hoang, Hoang Zung, and Ngo Huynh Buu Trong, “Structural properties of amorphous tio_2 nanoparticles,” *The European Physical Journal D* **44**, 515–524 (2007).
- ³² Rustam Z Khaliullin, Joost VandeVondele, and Jurg Hutter, “Efficient linear-scaling density functional theory for molecular systems,” *Journal of chemical theory and computation* **9**, 4421–4427 (2013).